Journal of Applied Sciences

ISSN 1812-5654

science alert

ANSInet
an open access publisher
http://ansinet.com

Journal of Applied Sciences 14 (9): 965-968, 2014
ISSN 1812-5654 / DOI: 10.3923/jas.2014.965.968

Structural and Optical Properties of ZnO Thin Films for Dye-Sensitized Solar Cell

H. Abdullah and N. Ariyanto
Department of Electrical, Electronics and Systems Engineering,
Faculty of Engineering and Built Environment,
Universiti Kebangsaan Malaysia, 43600, Bangi, Selangor, Malaysia

Abstract: The zinc oxide sol-gel was prepared as follows: Zinc acetate (M183.46. $Zn(C_2H_3O_2)_2$, 99.99% chemical purity) was first dissolved in iso propanol ($(CH_3)_2CHOH$) at room temperature. By using this method, the formation of zinc oxide film is much easier and cheaper to be prepared and it has been shown to achieve high breakdown fields by small grain size. Characterization of the zinc oxide is needed by using X-ray Diffraction (XRD), Scanning Electron Microscope (SEM) and Ultraviolet-Visible Spectroscopy (UV-Vis). XRD pattern shows the deposited films were polycrystalline with a hexagonal wurzite structure. Effect in concentration and thickness of zinc oxide will differ in the bandgap of the semiconductor. By doing this research, it is believe that zinc oxide has many advantages in solar cell application.

Key words: Zinc oxide, sol-gel method, thin film, porous, polycrystalline

INTRODUCTION

Among the wide range of one-dimensional (1D) semiconducting nano-materials, zinc oxide (ZnO) is a wide bandgap (3.3 eV at 298 K) semiconductor with a wurtzite crystal structure. Zinc oxide with high energy band gap of 3.35 eV and large exciton binding energy of 60 meV has been applied in wide range of applications from sensors to ultra-violet laser diodes and nanotechnology-based device (Cao *et al*., 2007). Mesoporous semiconductors offer great interest for their vast ability to adsorb and interact with atoms, ions and molecules on their wide interior surface and in the nanometer pore size (Charoensirithavorn and Yoshikawa, 2006). High surface area of porous zinc oxide has also been applied for gas sensor materials (Hariharan, 2006), biosensor (Huang *et al*., 2010), photocatalysts (Jagadish and Pearton, 2006) and photoelectrode of dye-sensitized solar cells (Jain *et al*., 2007). These ZnO nano-materials have received extensive interest for use in room-temperature ultraviolet lasing cavities, photodetectors, gas/chemical sensors, electronic devices and dye-sensitized solar cells (Kakiuchi *et al*., 2006). ZnO has been expected to be comparable to TiO_2 because of its higher electronic mobility, similar energy level of conduction band (Keis *et al*., 2002), conductive crystal structure due to anisotropic growth (Kumar and Chen, 2008) and its potential high-area film morphologies (Law *et al*., 2005). ZnO is a versatile material that has a diverse group of morphologies such as nanocombs, nanorings, nanobelts, nanorods and nanowires. Experiment shows a promising 5% efficiency from ZnO. Compared with the nanoparticle ZnO films, ZnO films containing vertically-aligned nanorods ZnO film favor the electron transport due to the smoother electron transport channels and longer electron diffusion (Liao *et al*., 2008). Theoretically the vertically-aligned structure provides a more direct path to the conductive glass electrode combined with fewer sites for trapping electrons (Law *et al*., 2005). In this study, we prepared a thin film by using sol-gel tecnique and inexpensive source materials such as zinc acetate dihydrate, ethylene glycol, iso-propanol and methanol solution. Moreover, structural, microstructure and optical characteristics of ZnO thin films were investigated.

MATERIALS AND METHODS

Substrate that used in the experiment is FTO that is SnO_2:F. It is cut into a size of 2×2 cm. The substrate is cleaned in beaker containing acetone solution using ultrasonic vibrator. The process is repeated by using isopropanol and methanol solution. The zinc oxide sol-gel was prepared by dissolving zinc acetate in isopropanol at room temperature and MEA was added as stabilizer. The resulting mixture was then stirred at 80°C for 1 h to form a clear and transparent homogeneous mixture and upon cooling was filtered to remove away foreign particulates. The mixture was aged for 24 h at room temperature.

Corresponding Author: H. Abdullah, Department of Electrical, Electronics and Systems Engineering, Faculty of Engineering and Built Environment, Universiti Kebangsaan Malaysia, 43600, Bangi, Selangor, Malaysia

Zinc oxide thin films were prepared by spin coating at rotation speed of 2500 rpm for 30 sec. The substrates were dried on a hotplate at 100°C for 1 h before placed in furnace for annealing at 600°C. The processes are repeated to get a thicker film. The degree of crystallinity and crystalline orientation of the zinc oxide thin films was measured using a Siemens (D-500) X-ray diffractometer (XRD) in the 2θ range between 10-80°. Optical transmittance spectra were recorded using a Jasco UV-Vis-NIR 3102-PC spectrophotometer over the wavelength range between 200 and 800 nm. The surface morphology and the thickness of the films were evaluated using a Philips Scan XL30 scanning electron microscope.

RESULTS AND DISCUSSION

Figure 1 shows X-ray Diffraction patterns and from graphs shows that the deposited films were polycrystalline with a hexagonal wurzite structure (Martinson *et al*., 2006). There are two peaks in the graph where there are both having different angles of diffraction and peak intensity. From the database, it seems that the two zinc oxides have different parameters.

Still they have the same orientation that is (002) although the difference in concentration (Ariyanto *et al*., 2009). The first peak that is indicating in blue colour is the hexagonal zinc oxide. The diffraction peak appears at 31.8° while the diffraction peak in red is appearing at 33.4°. This material is known as zincite which has the same molecular structure and orientation of the zinc oxide. Table 1 shows the properties in difference between the two zinc oxides.

The optical absorption spectra of the sol-gel deposited ZnO films in the UV-Visible wavelength range of 200-800 nm are presented in Fig. 2 with different concentrations (0.5 and 0.8 mol L^{-1}) different thicknesses (10 and 15 layers). By comparing within the difference in concentration, the absorption ratio becomes larger when there is an increase in concentration. For the 0.8 M 15 layers graph, it is much lower compare to the 0.5 M 15 layers. As a result, it can be concluded that the higher the concentration, the much light transmits through the sample. By comparing the number of layers, the 0.5 M 10 layers have a lower graph compare to 0.5 M 15 layers. All the ZnO samples exhibit an intrinsic absorption with similar absorption intensity below 390 nm, caused by the ZnO semiconductor with electron transfer from the valence band to the conduction band (Suh *et al*., 2007).

We can derive and obtain the effective band gap (E_g) from the data used in the plot the graph of UV-Vis spectra. The values of absorption coefficient are calculated using Eq. 1:

$$It = I_o \exp(-\alpha t) \quad (1)$$

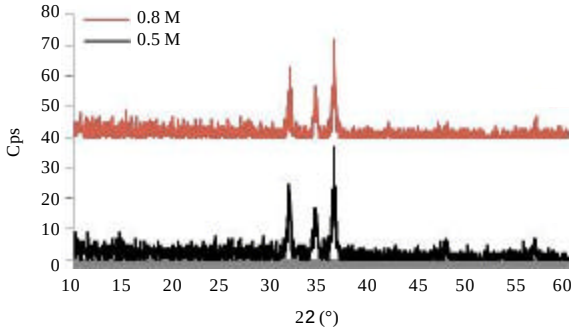

Fig. 1: X-ray Diffraction pattern of ZnO colloid thin film

Table 1: Parameter difference between polycrystalline zinc oxide and Zincite.

Material	Zinc oxide, ZnO	Zincite, ZnO
Structure	Hexagonal	Hexagonal
Parameter a (Å)	3.24986	3.24200
Parameter b (Å)	3.24986	3.24200
Parameter c (Å)	5.20662	5.17600
Distance between atom, d (Å)	2.80949	2.48578
Angle, 2θ	31.826°	36.407°
Peak intensity	13.9567	19.2365

Table 2: Effects on the concentration and thickness on the optical bandgap of ZnO thin films

Sample types	Optical band gap (eV)
0.5 M 10 layers	3.27
0.5 M 15 layers	3.23
0.8 M 10 layers	3.34
0.8 M 15 layers	3.30

where, α is the optical absorption coefficient, t is the thickness of the film, I_t and I_o are the intensity of transmitted light and initial light, respectively. We can further simplify the equation since the transmittance, T is known as:

$$T = It/Io \quad (2)$$

The absorption coefficient (α) is related to the incident photon energy as:

$$\alpha = K (hv-E_g)^{n/2}/hv \quad (3)$$

where, K is constant, E_g is the energy gap and n is constant equal to 1 for direct gap compound. The band gap values are measured by extrapolating the straight-line portion over the hv axis. The predetermined band gap values are listed in Table 2. From the Table 2, we can observe that the band gap of ZnO within the thicker layer has a decrease in band gap. This means the lower the band gap the probability for an electron to pass through the band gap is much higher.

Figure 3 shows SEM images for ZnO colloid thin film deposited on the FTO substrate in order to study the thin

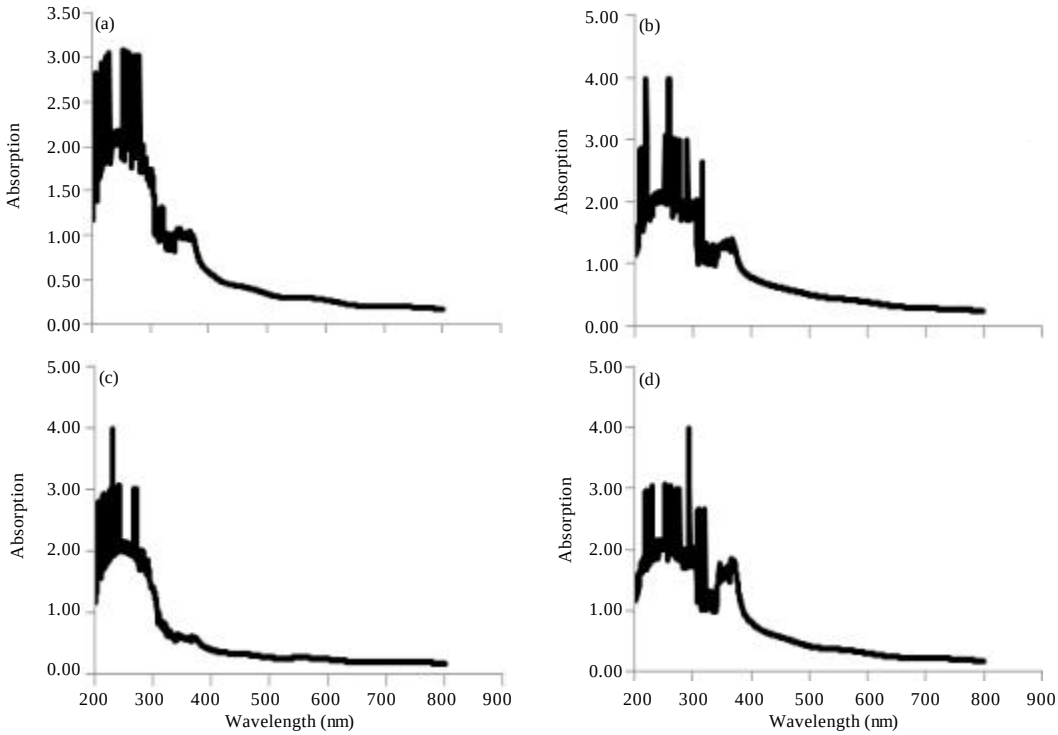

Fig. 2(a-c): UV-Vis spectra with (a) 0.5 M 10 layers, (b) 0.5 M 15 layers, (c) 0.8 M 10 layers and (d) 0.8 M 15 layers

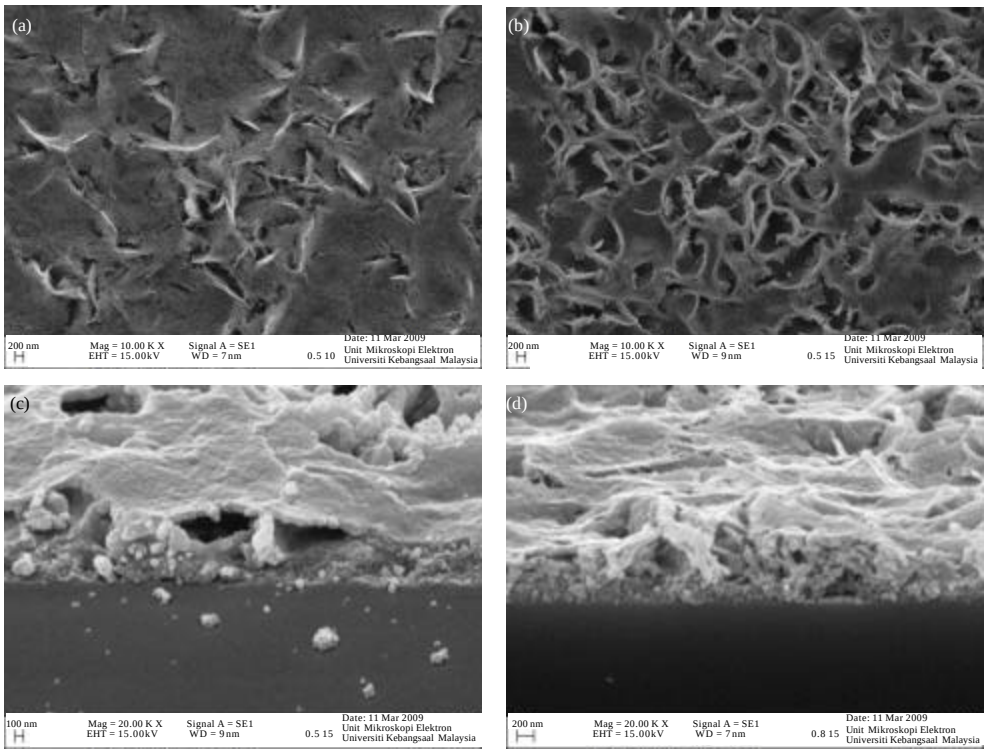

Fig. 3(a-d): Photographs from SEM where (a) Top view of sample 0.5 M 10 layers, (b) Top view of sample 0.5 M 15 layers, (c) Side view of sample 0.5 M 15 layers and (d) Side view of sample 0.8 M 15 layers

film surface. From Fig. 3a-d shows that as the film thickness increased, the deeper layers of atoms are subjected to form a compact structure, stronger interatomic forces and otherwise for thin films thus form a spongy loose packed structure (Zhang *et al*., 2009). The porous structure is needed to increase the surface area in order to increase the probability of electron flow through the thin film and out to the external circuit. The thickness of the 10 layers sample varies from 100-400 nm where as the 15 layers is around 600-900 nm. The size of the porous is around 60-90 nm.

CONCLUSION

Zinc oxides thin films were fabricated from sol-gels prepared with 0.5 and 0.8 M zinc acetate concentration. Thin film thickness was measured and ranged within 100-400 nm for 10 layers and 600-900 nm for 15 layers. Crack-free films or porous structure was obtained in the four samples. In the analysis of XRD, it is found that all of the samples had a hexagonal wurzite structure. The band gap for ZnO ranged from 3.16 to 3.34 eV depending on the concentration and the thickness of the thin film. The high anneal temperature resulted in the higher of transmittance of the infrared spectra.

REFERENCES

Ariyanto, N.P., H. Abdullah, S. Shaari, S. Junaidi and B. Yuliarto, 2009. Preparation and characterisation of porous nanosheets zinc oxide films: Based on chemical bath deposition. World Applied Sci. J., 6: 764-768.

Cao, B., X. Teng, S.H. Heo, Y. Li, S.O. Cho, G. Li and W. Cai, 2007. Different ZnO nanostructures fabricated by a seed-layer assisted electrochemical route and their photoluminescence and field emission properties. J. Phys. Chem. C, 111: 2470-2476.

Charoensirithavorn, P. and S. Yoshikawa, 2006. Dye-sensitized solar cell based on ZnO nanorod arrays. Proceedings of the 2nd Joint International Conference on Sustainable Energy and Environment, November 21-23, 2006, Bangkok, Thailand, pp: 21-23.

Hariharan, C., 2006. Photocatalytic degradation of organic contaminants in water by ZnO nanoparticles: Revisited. Revisite. Applied Catalysis A: General, 304: 55-61.

Huang, C.J., W.K. Chao and F.S. Shieu, 2010. Characteristics of zinc oxide crystallites deposited on ITO for dye-sensitized solar cells. J. Chin. Chem. Soc., 57: 1200-1203.

Jagadish, C. and S.J. Pearton, 2006. Zinc Oxide Bulk, Thin Film and Nanostructures: Processing, Properties and Applications. Elsevier, Amsterdam, ISBN-13: 9780080464039, Pages: 600.

Jain, A., P. Sagar and R.M. Mehra, 2007. Changes of structural, optical and electrical properties of sol-gel derived ZnO films with their thickness. Mater. Sci. Poland, 25: 233-242.

Kakiuchi, K., E. Hosono and S. Fujihara, 2006. Enhanced photoelectrochemical performance of ZnO electrodes sensitized with N-719. J. Photochem. Photobiol. A: Chem., 179: 81-86.

Keis, K., C. Bauer, G. Boschloo, A. Hagfeldt, K. Westermark, H. Rensmo and H. Siegbahn, 2002. Nanostructured ZnO electrodes for dye-sensitized solar cell applications. J. Photochem. Photobiol. A: Chem., 148: 57-64.

Kumar, S.A. and S.M. Chen, 2008. Nanostructured zinc oxide particles in chemically modified electrodes for biosensor applications. Anal. Lett., 41: 141-158.

Law, M., L.E. Greene, J.C. Johnson, R. Saykally and P. Yang, 2005. Nanowire dye-sensitized solar cells. Nat. Mater., 4: 455-459.

Liao, L., H.B. Lu, M. Shuai, J.C. Li and Y.L. Liu *et al*., 2008. A novel gas sensor based on field ionization from ZnO nanowires: M oderate working voltage and high stability. Nanotechnology, Vol. 19. 10.1088/0957-4484/19/17/175501

Martinson, A.B.F., J.E. McGarrah, M.O.K. Parpia and J.T. Hupp, 2006. Dynamics of charge transport and recombination in ZnO nanorod array dye-sensitized solar cells. Phys. Chem. Chem. Phys., 8: 4655-4659.

Suh, D.I., S.Y. Lee, T.H. Kim, J.M. Chun, E.K. Suh, O.B. Yang and S.K. Lee, 2007. The fabrication and characterization of dye-sensitized solar cells with a branched structure of ZnO nanowires. Chem. Phys. Lett., 442: 348-353.

Zhang, Q., C.S. Dandeneau, X. Zhou and G. Cao, 2009. ZnO nanostructures for dye-sensitized solar cells. Adv. Mater., 21: 4087-4108.